

Reaction, Lévy Flights, and Quenched Disorder

Ligang Chen and Michael W. Deem

Department of Chemical Engineering, University of California, Los Angeles, CA 90095-1592

We consider the $A + A \rightarrow \emptyset$ reaction, where the transport of the particles is given by Lévy flights in a quenched random potential. With a common literature model of the disorder, the random potential can only increase the rate of reaction. With a model of the disorder that obeys detailed balance, however, the rate of reaction initially increases and then decreases as a function of the disorder strength. The physical behavior obtained with this second model is in accord with that for reactive turbulent flow, indicating that Lévy flight statistics can model aspects of turbulent fluid transport.

05.40.Fb, 82.20.Mj, 05.60.Cd

I. INTRODUCTION

Lévy flights have been used to model a variety of physical processes such as epidemic spreading [1], self-diffusion in micelle systems [2], and transport in heterogeneous rocks [3]. Lévy flights are essentially a generalization of ordinary Brownian walks. The normalized step size distribution for Lévy flights in d dimensions is

$$p(r)d^d r = \frac{f r_0^f}{S_d} r^{-1-f} dr d\Omega \quad (1)$$

where r is the step size, f is the step index, $S_d = 2\pi^{d/2}/(d/2 - 1)!$, and r_0 a lower microscopic step cut-off. In the case of $f = 2$, we recover Brownian motion. However, for $f < 2$, the distribution of step sizes exhibits a long-range algebraic tail that corresponds to large but infrequent steps, so called *rare events*. Due to these rare, large steps, the mean square step size deviation diverges, and the central limit theorem does not hold. The rare, large step events prevail and determine the long time behavior. The dynamic exponent z that characterizes the mean square displacement as a function of time by $\langle r^2(t) \rangle \sim (\text{const})t^{2/z}$ depends on the microscopic step index f according to the relationship $z = f$, indicating anomalous enhanced diffusion, that is, superdiffusion.

It is well-known that quenched random disorder leads to sub-diffusive behavior in two-dimensional Brownian walks. Lévy flights in such random environments have attracted increasing attention recently. The interplay between the “built-in” superdiffusive behavior of the Lévy flights and the effect of the random environment generally leading to sub-diffusive behavior has been examined [4–6]. Surprisingly, in the models of random disorder examined to date, the dynamic exponent z locks into the Lévy flight index f , regardless of the strength of disorder.

The behavior of chemical reactions with random potential [7,8] and isotropic turbulence disorder [9,10] has been examined. Reactants diffusing according to Lévy flight statistics have also been studied in a model of branching and annihilating processes [11]. In general, potential disorder tends to slow down the diffusing reactants. Since these reactions typically become transport-limited

at long times, potential disorder tends to slow down the reaction as well. But, it was found that a small amount of potential disorder added to the turbulent fluid mixing leads to an increased rate of reaction. This phenomenon of ‘superfast’ reaction occurs because the disorder traps reactants in local potential wells, which quadratically increases the local reaction rate, while the turbulence rapidly replenishes the reacting species to these regions. As the potential disorder is increased, eventually the rate of reaction decreases, due to a slowing of the transport. It is interesting to study the behavior of reactants following Lévy flight statistics in quenched random disorder. The question is: Can the Lévy statistics mimic rapid turbulent transport and so lead to superfast reaction? Furthermore, do the reactions become transport limited or reaction limited at long times?

In this paper, we analyze two different models of the disorder. A conventional literature model, which does not satisfy detailed balance, is discussed in section II. A new model that does satisfy detailed balance is discussed in section III. We study the effect of Lévy flight statistics and quenched random disorder on the simple bimolecular recombination reaction in two dimensions. Detailed results of the field theoretic renormalization are presented. We conclude this paper in section IV.

II. REACTION IN A COMMON LITERATURE MODEL OF DISORDER

Including the normal diffusion term, the Fokker-Plank equation for Lévy flights in a quenched potential field has been modeled by [4–6]

$$\begin{aligned} \frac{\partial P(\mathbf{r}, t)}{\partial t} = & D_2 \nabla^2 P(\mathbf{r}, t) + D_f (\nabla^2)^{f/2} P(\mathbf{r}, t) \\ & + \nabla \cdot [P(\mathbf{r}, t) \nabla V(\mathbf{r})] \end{aligned} \quad (2)$$

where, $(\nabla^2)^{f/2}$ is interpreted as the inverse Fourier transform of $-k^f$, which is a spatially non-local integral operator reflecting the long-range character of the Lévy steps with microscopic step index f . Fourier transforms are defined as $\hat{f}(\mathbf{k}) = \int d^d x e^{i\mathbf{k} \cdot \mathbf{x}} f(\mathbf{x})$. The last term on the

right hand side is a drift term due to the motion of the walker in the force field. We assume a Gaussian distribution of the random potential force field, $V(\mathbf{r})$, with correlation

$$\langle V(\mathbf{k}_1)V(\mathbf{k}_2) \rangle = \frac{\gamma}{k^{2+y}} (2\pi)^d \delta(\mathbf{k}_1 + \mathbf{k}_2) \quad (3)$$

The reaction we are considering is

$$A + A \xrightarrow{\lambda} \emptyset \quad (4)$$

A field theory is derived by identifying a master equation and using the coherent state mapping [12]. The random potential is incorporated with the replica trick [13]. The action within the field theory is

$$\begin{aligned} S = & \int d^d \mathbf{x} \int_0^{t_f} dt \bar{a}_i(\mathbf{x}, t) [\partial_t - D_f(\nabla^2)^{f/2} - D_2 \nabla^2 \\ & + \delta(t)] a_i(\mathbf{x}, t) + \frac{\lambda}{2} \int d^d \mathbf{x} \int_0^{t_f} dt [2\bar{a}_i(\mathbf{x}, t) a_i^2(\mathbf{x}, t) \\ & + \bar{a}_i^2(\mathbf{x}, t) a_i^2(\mathbf{x}, t)] - n_0 \int d^d \mathbf{x} \bar{a}_i(\mathbf{x}, 0) \\ & - \frac{\gamma}{2} \int dt_1 dt_2 \int_{\mathbf{k}_1 \mathbf{k}_2 \mathbf{k}_3 \mathbf{k}_4} (2\pi)^d \delta(\mathbf{k}_1 + \mathbf{k}_2 + \mathbf{k}_3 + \mathbf{k}_4) \\ & \times \frac{\mathbf{k}_1 \cdot (\mathbf{k}_1 + \mathbf{k}_2) \mathbf{k}_3 \cdot (\mathbf{k}_3 + \mathbf{k}_4)}{|\mathbf{k}_1 + \mathbf{k}_2|^{2+y}} \\ & \times \hat{a}_i(\mathbf{k}_1, t_1) \hat{a}_i(\mathbf{k}_2, t_1) \hat{a}_j(\mathbf{k}_3, t_2) \hat{a}_j(\mathbf{k}_4, t_2) \end{aligned} \quad (5)$$

Summation is implied over replica indices. The notation $\int_{\mathbf{k}}$ stands for $\int d^d \mathbf{k} / (2\pi)^d$.

The concentration of the reactant A at time t , averaged over the initial conditions, is given by

$$c_A(\mathbf{x}, t) = \lim_{N \rightarrow 0} \langle a_i(\mathbf{x}, t) \rangle \quad (6)$$

where the average is taken with respect to $\exp(-S)$.

To apply the field theoretic renormalization procedure, the action is recast [14] as

$$\begin{aligned} S = & \int d^d \mathbf{x} \int_0^{t_f} dt \bar{a}_i(\mathbf{x}, t) [\partial_t - Z_f D_{fR}(\nabla^2)^{f/2} \\ & - \mu^{f-2} Z_2 D_{2R} D_{fR} \nabla^2 + \delta(t)] a_i(\mathbf{x}, t) \\ & + \frac{1}{2} \mu^{f-d} Z_\lambda \lambda_R D_{fR} \int d^d \mathbf{x} \int_0^{t_f} dt [2\bar{a}_i(\mathbf{x}, t) a_i^2(\mathbf{x}, t) \\ & + \bar{a}_i^2(\mathbf{x}, t) a_i^2(\mathbf{x}, t)] - \mu^d n_{0R} \int d^d \mathbf{x} \bar{a}_i(\mathbf{x}, 0) \\ & - \frac{1}{2} \mu^\epsilon Z_\gamma \gamma_R D_{fR}^2 \int dt_1 dt_2 \int_{\mathbf{k}_1 \mathbf{k}_2 \mathbf{k}_3 \mathbf{k}_4} (2\pi)^d \\ & \times \delta(\mathbf{k}_1 + \mathbf{k}_2 + \mathbf{k}_3 + \mathbf{k}_4) \frac{\mathbf{k}_1 \cdot (\mathbf{k}_1 + \mathbf{k}_2) \mathbf{k}_3 \cdot (\mathbf{k}_3 + \mathbf{k}_4)}{|\mathbf{k}_1 + \mathbf{k}_2|^{2+y}} \\ & \times \hat{a}_i(\mathbf{k}_1, t_1) \hat{a}_i(\mathbf{k}_2, t_1) \hat{a}_j(\mathbf{k}_3, t_2) \hat{a}_j(\mathbf{k}_4, t_2) \end{aligned} \quad (7)$$

where the renormalization constants Z_f , Z_2 , Z_λ , and Z_γ have been introduced to absorb the UV divergences of the

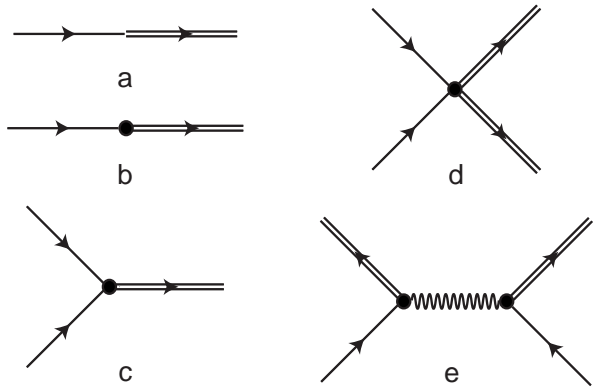


FIG. 1. (a) Full lines represent the propagator, and the arrow points in the direction of increasing time. (b) Normal diffusion vertex D_2 . (c), (d) Reaction vertices λ . (e) Disorder vertex γ .

model. The parameters, D_{fR} , D_{2R} , λ_R , and γ_R are the dimensionless expansion parameters of the model. Since the Lévy flight term, $D_{fR}(\nabla^2)^{f/2}$, is the most important term, it is chosen as the dimensionless free term, i.e. the propagator is $[\partial_t - D_{fR}(\nabla^2)^{f/2}]^{-1}$. Note, we are not allowed to treat the regular diffusion term as free term, as this violates the physics of the scaling and leads to a diverging renormalized D_f . Now, the standard critical dimension of γ_R is $d_c = 2f + y - 2$, and we introduce for an ϵ expansion $\epsilon = d_c - d$. The wave-number scale-setting parameter is denoted by μ , and we assign the dimensions to the rest of the terms accordingly.

The connections between the renormalized and unrenormalized parameters are

$$\begin{aligned} Z_f D_{fR} &= D_f \\ \mu^{f-2} Z_2 D_{2R} D_{fR} &= D_2 \\ \mu^{f-d} Z_\lambda \lambda_R D_{fR} &= \lambda \\ \mu^d n_{0R} &= n_0 \\ \mu^\epsilon Z_\gamma \gamma_R D_{fR}^2 &= \gamma \end{aligned} \quad (8)$$

To one-loop order, self-energy diagrams and vertex diagrams are summarized in Fig. 1 and Fig. 2. We may be tempted to use the momentum-shell renormalization procedure here. However, due to the difficulty of regularizing this action, the first self-energy diagram would incorrectly contribute to D_{2R} by the momentum-shell renormalization, rather than to D_{fR} by the field theoretic renormalization that is consistent with perturbation theory. In the evaluation of the diagram in Fig. 2a, it is important to treat the external momentum exactly. If a series expansion in the external momentum is performed on the integrand, rather than on the result of the integral, an incorrect contribution to Z_2 arises. Interestingly, when the diagram in Fig. 2a is evaluated, only a finite contribution to Z_f results. Complete calculation shows

$$Z_f = 1$$

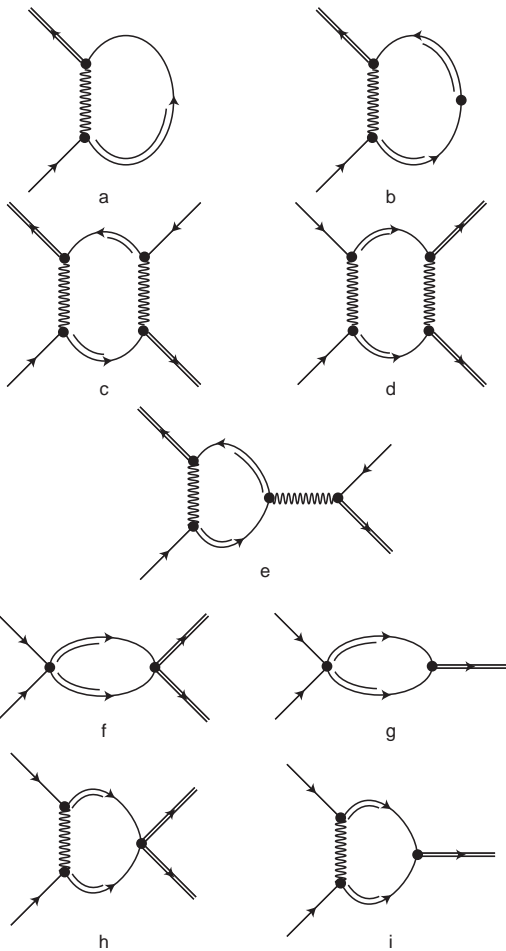


FIG. 2. One-loop diagrams: (a) self-energy diagram contributing to D_f ; (b) self-energy diagram contributing to D_2 ; (c), (d), and (e) vertex diagrams contributing to γ ; (f), (g), (h), and (i) vertex diagrams contributing to λ .

$$\begin{aligned} Z_2 &= 1 - \frac{(2f-3)\gamma}{4\pi\epsilon} \\ Z_\lambda &= 1 - \frac{\gamma_R}{2\pi\epsilon} + \frac{\lambda_R}{4\pi(f-d)} \\ Z_\gamma &= 1 + \frac{\gamma_R}{2\pi\epsilon} \end{aligned} \quad (9)$$

where a double pole expansion, $1/\epsilon$ and $1/(f-d)$, is used in the calculation of Z_λ . The use of the double pole expansion in two dimensions means we consider f just slightly smaller than 2 and y small. As usual, the β functions defined by

$$\begin{aligned} \beta_{D_{2R}} &= \mu \frac{\partial}{\partial \mu} D_{2R} \\ \beta_{\lambda_R} &= \mu \frac{\partial}{\partial \mu} \lambda_R \\ \beta_{\gamma_R} &= \mu \frac{\partial}{\partial \mu} \gamma_R \end{aligned} \quad (10)$$

give the flow equations in two dimensions as

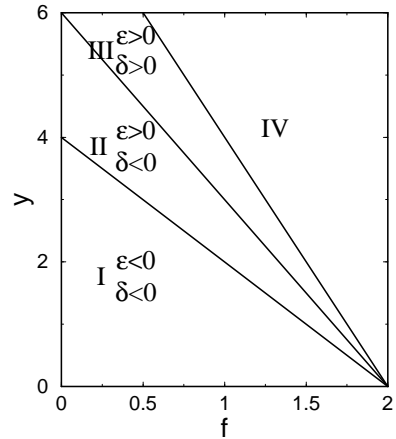


FIG. 3. Different regions predicted by the flow equations for the Lévy flight system with disorder model I. The flow equations are accurate for small y and f slightly less than 2. The flow equations do not apply in region IV.

$$\begin{aligned} \frac{dD_{2R}}{dl} &= -\beta_{D_{2R}} = (f-2)D_{2R} + \frac{(2f-3)\gamma_R D_{2R}}{4\pi} \\ \frac{d\lambda_R}{dl} &= -\beta_{\lambda_R} = (f-2)\lambda_R + \frac{\gamma_R \lambda_R}{2\pi} - \frac{\lambda_R^2}{4\pi} \\ \frac{d\gamma_R}{dl} &= -\beta_{\gamma_R} = \epsilon\gamma_R - \frac{\gamma_R^2}{2\pi} \end{aligned} \quad (11)$$

where we use the relation $\mu = \Lambda/e^l$, and Λ is a microscopic cutoff. Since $Z_f = 1$, the reaction and disorder terms do not affect the dynamic exponent, and $z = f$. We determine the long-time decay from the flow equation via matching to short-time perturbation theory. The flow equations are integrated to a short time such that

$$t(l^*) = t \exp[- \int_0^{l^*} z(l) dl] = t_0 \quad (12)$$

At short times, we find the mean square displacement of an unreactive particle from $\langle r^2(t(l^*), l^*) \rangle = 4D_f t(l^*)$, and the concentration of reactants from $c_A(t(l^*), l^*) = [(n_{0R}(l^*)\Lambda^d)^{-1} + D_f \lambda_R(l^*)\Lambda^{d-2} t(l^*)]^{-1}$. The long-time asymptotic values are given by scaling: $\langle r^2(t) \rangle = e^{2l^*} \langle r^2(t(l^*), l^*) \rangle$, and $c_A(t) = e^{-2l^*} c_A(t(l^*), l^*)$.

We first investigate the behavior of D_{2R} . As we will see below, the fixed point for γ_R is $\max(0, 2\pi\epsilon)$. Using this result, we see that D_{2R} flows exponentially to zero as long as $y < 4(2-f)$, when f is near 2. Likely, a higher loop calculation would extend the region in which D_{2R} flows to zero. Thus, at least within the region in which our flow equations apply, D_{2R} always flows to 0 in the presence of Lévy flights. It is, therefore, unnecessary to introduce such a normal diffusion term in the model.

For $\epsilon < 0$, i.e. in region I of Fig. 3, there is only a set of trivial stable fixed points, $\gamma_R^* = 0$ and $\lambda_R^* = 0$, for the system. The matching procedure gives the normal concentration decay as

$$c_A(t) \sim \frac{1}{\lambda t} \quad (13)$$

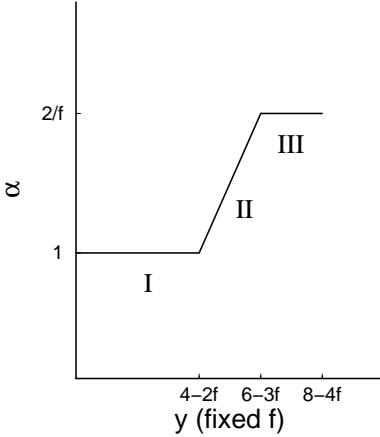


FIG. 4. Decay exponent for the $A + A \rightarrow \emptyset$ reaction in the Lévy flight system with disorder model I: $c_A(t) \sim (\text{const})t^{-\alpha}$.

In the region of $\epsilon > 0$, $\gamma_R^* = 2\pi\epsilon$ is the nontrivial fixed point. But depending on the value of $\delta = 3f + y - 6$, the matching procedure yields different results. For $\delta < 0$, i.e. in region II of Fig. 3, there is no nontrivial fixed point for λ_R . The corresponding asymptotic concentration decay is a little faster than that in region I:

$$c_A(t) \sim \frac{1}{t_0} \left(\frac{1}{\lambda} + \frac{1}{4\pi|\delta|D_f\Lambda^{f-2}} \right) \left(\frac{t}{t_0} \right)^{-\frac{2-|\delta|}{f}} \quad (14)$$

For $\delta > 0$, i.e. in region III of Fig. 3, $\lambda_R^* = 4\pi\delta$ is the fixed point. The asymptotic concentration decay is the fastest:

$$c_A(t) \sim \frac{1}{4\pi\delta D_f \Lambda^{f-2} t_0} \left(\frac{t}{t_0} \right)^{-\frac{2}{f}} \quad (15)$$

The relationship between the concentration decay exponent, α , and disorder strength, y , at fixed value of f is plotted in Fig 4. Note that the strength of the disorder has no effect on the decay exponent, affecting only the prefactor.

The reader may note that the disorder can never slow down the reaction in this model. This is quite an unexpected result, as these reactions are expected to become transport-limited at long times, and disorder should slow down the transport. Model I, Eq. (2), is somewhat unphysical in that this cannot happen due to the lack of disorder contribution to Z_f .

III. REACTION IN A MODEL OF DISORDER THAT OBEYS DETAILED BALANCE

Although Eq. (2) is often used in the literature, it does not guarantee a long-time Boltzmann distribution for $P(\mathbf{r}, t)$. That is, this form of the disorder does not satisfy detailed balance. A more natural form of the Fokker-Plank equation for Lévy flights in random disorder is

$$\frac{\partial P(\mathbf{r}, t)}{\partial t} = \nabla^{f-1} \cdot [D_f \nabla P(\mathbf{r}, t) + P(\mathbf{r}, t) \nabla V(\mathbf{r})] \quad (16)$$

where ∇^{f-1} is the inverse Fourier transform of $-ik^{f-2}\mathbf{k}$. Equation (16) can, alternatively, be interpreted as a modification of the continuity equation to take into account the long-range transport induced by the Lévy flights. With the same form of the correlation function for the potential, Eq. (3), we have

$$\begin{aligned} S = & \int d^d \mathbf{x} \int_0^{t_f} dt \bar{a}_i(\mathbf{x}, t) [\partial_t - D_f (\nabla^2)^{f/2} + \delta(t)] a_i(\mathbf{x}, t) \\ & + \frac{\lambda}{2} \int d^d \mathbf{x} \int_0^{t_f} dt [2\bar{a}_i(\mathbf{x}, t) a_i^2(\mathbf{x}, t) + \bar{a}_i^2(\mathbf{x}, t) a_i^2(\mathbf{x}, t)] \\ & - n_0 \int d^d \mathbf{x} \bar{a}_i(\mathbf{x}, 0) \\ & - \frac{\gamma}{2} \int dt_1 dt_2 \int_{\mathbf{k}_1 \mathbf{k}_2 \mathbf{k}_3 \mathbf{k}_4} (2\pi)^d \delta(\mathbf{k}_1 + \mathbf{k}_2 + \mathbf{k}_3 + \mathbf{k}_4) \\ & \times \frac{k_1^{f-2} k_3^{f-2} \mathbf{k}_1 \cdot (\mathbf{k}_1 + \mathbf{k}_2) \mathbf{k}_3 \cdot (\mathbf{k}_3 + \mathbf{k}_4)}{|\mathbf{k}_1 + \mathbf{k}_2|^{2+y}} \\ & \times \hat{a}_i(\mathbf{k}_1, t_1) \hat{a}_i(\mathbf{k}_2, t_1) \hat{a}_j(\mathbf{k}_3, t_2) \hat{a}_j(\mathbf{k}_4, t_2) \end{aligned} \quad (17)$$

Again, to apply the field theoretic renormalization procedure, the action is recast as

$$\begin{aligned} S = & \int d^d \mathbf{x} \int_0^{t_f} dt \bar{a}_i(\mathbf{x}, t) [\partial_t - Z_f D_{fR} (\nabla^2)^{f/2} \\ & + \delta(t)] a_i(\mathbf{x}, t) + \frac{1}{2} \mu^{f-d} Z_\lambda \lambda_R D_{fR} \int d^d \mathbf{x} \int_0^{t_f} dt \\ & \times [2\bar{a}_i(\mathbf{x}, t) a_i^2(\mathbf{x}, t) + \bar{a}_i^2(\mathbf{x}, t) a_i^2(\mathbf{x}, t)] \\ & - \mu^d n_{0R} \int d^d \mathbf{x} \bar{a}_i(\mathbf{x}, 0) - \frac{1}{2} \mu^\epsilon Z_\gamma \gamma_R D_{fR}^2 \int dt_1 dt_2 \\ & \times \int_{\mathbf{k}_1 \mathbf{k}_2 \mathbf{k}_3 \mathbf{k}_4} (2\pi)^d \delta(\mathbf{k}_1 + \mathbf{k}_2 + \mathbf{k}_3 + \mathbf{k}_4) \\ & \times \frac{k_1^{f-2} k_3^{f-2} \mathbf{k}_1 \cdot (\mathbf{k}_1 + \mathbf{k}_2) \mathbf{k}_3 \cdot (\mathbf{k}_3 + \mathbf{k}_4)}{|\mathbf{k}_1 + \mathbf{k}_2|^{2+y}} \\ & \times \hat{a}_i(\mathbf{k}_1, t_1) \hat{a}_i(\mathbf{k}_2, t_1) \hat{a}_j(\mathbf{k}_3, t_2) \hat{a}_j(\mathbf{k}_4, t_2) \end{aligned} \quad (18)$$

where, $d_c = 2 + y$, $\epsilon = d_c - d$, and the rest of the parameters are the same as in action I.

The connections between the renormalized and unrenormalized parameters are

$$\begin{aligned} Z_f D_{fR} &= D_f \\ \mu^{f-d} Z_\lambda \lambda_R D_{fR} &= \lambda \\ \mu^d n_{0R} &= n_0 \\ \mu^\epsilon Z_\gamma \gamma_R D_{fR}^2 &= \gamma \end{aligned} \quad (19)$$

The diagrams are the same as those in Figs. 1 and 2, except that the diagrams from normal diffusion, Figs. 1b and 2b, are not present. A one-loop diagrammatic calculation gives

$$\begin{aligned}
Z_f &= 1 + \frac{\gamma_R}{4\pi\epsilon} \\
Z_\lambda &= 1 - \frac{\gamma_R}{2\pi\epsilon} + \frac{\lambda_R}{4\pi(f-d)} \\
Z_\gamma &= 1 + \frac{\gamma_R}{2\pi\epsilon}
\end{aligned} \tag{20}$$

where a double-pole expansion of $1/\epsilon$ and $1/(f-d)$ is used in the calculation of Z_λ .

The dynamic exponent is given by

$$z = f - \mu \frac{\partial}{\partial \mu} \ln Z_f = f + \frac{\gamma_R}{4\pi} \tag{21}$$

This suggests that the Lévy flights are significantly slowed by the presence of the new random disorder term. That is, when detailed balance is obeyed, the disorder affects the dynamical exponent.

The β functions give us the flow equations from Z_i in two dimensions as

$$\begin{aligned}
\frac{d\lambda_R}{dl} &= -\beta_{\lambda_R} = (f-2)\lambda_R + \frac{3\gamma_R\lambda_R}{4\pi} - \frac{\lambda_R^2}{4\pi} \\
\frac{d\gamma_R}{dl} &= -\beta_{\gamma_R} = \epsilon\gamma_R
\end{aligned} \tag{22}$$

This action is well-behaved, and there is no regularization difficulty. And indeed, both momentum-shell renormalization and theoretic renormalization yield identical flow equations to one-loop order. From the flow equations, for $\epsilon > 0$, γ_R flows to ∞ , indicating that the disorder dominates over the Lévy flights. For $\epsilon < 0$, γ_R flows to 0, indicating transport of Lévy flights dominates over the disorder. This same behavior, that the disorder must be adjusted to be compatible with the transport, was found in the turbulent reactive flow problem [10]. An interesting system arises when those two effects are competitive, and so we require $\epsilon = 0$, i.e. $y = 0$. Under this constraint, $\gamma_R = \gamma/D_f^2$ does not flow. Very likely, this result holds to all orders. Further analysis of the flow equation for λ_R indicates two regimes. For $\gamma/D_f^2 > 4(2-f)\pi/3$, or strong disorder, λ_R has a stable nontrivial fixed point, given by

$$\lambda_R^* = 4\pi(f-2) + \frac{3\gamma}{D_f^2} = \lambda^* \Lambda^{2-f}/D_f \tag{23}$$

Following the matching procedure, we have

$$c_A(t) \sim \frac{1}{\lambda^* t} \left(\frac{t}{t_0} \right)^{-\frac{2}{f+\gamma/(4\pi D_f^2)} + 1} \tag{24}$$

However, for $\gamma/D_f^2 < 4(2-f)\pi/3$, or weak disorder, there is no nontrivial fixed point for λ_R , and we have

$$\begin{aligned}
c_A(t) &\sim \left(\frac{1}{\lambda} + \frac{1}{[4\pi(2-f) - 3\gamma/D_f^2]\Lambda^{f-2}D_f} \right) \\
&\times \frac{1}{t} \left(\frac{t}{t_0} \right)^{-\frac{\gamma/(2\pi D_f^2)}{f+\gamma/(4\pi D_f^2)}}
\end{aligned} \tag{25}$$

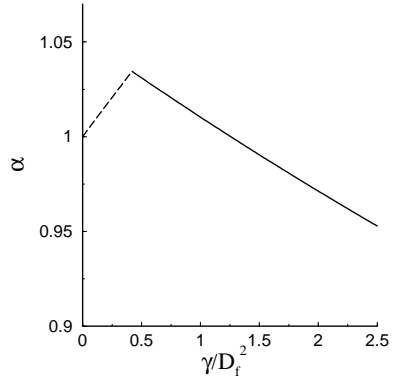


FIG. 5. Decay exponent for the $A + A \rightarrow \emptyset$ reaction in the Lévy flight system that obeys detailed balance: $c_A(t) \sim (\text{const})t^{-\alpha}$. The figure is shown for $f = 1.9$. The reaction is transport limited on the solid curve and reaction limited on the dashed curve. Note that the region $\alpha > 1$ corresponds to 'superfast' reaction.

For the special case of $\gamma/D_f^2 = 4(2-f)\pi/3$, λ_R decays marginally, and we have a logarithmic correction to the decay:

$$c_A(t) \sim \frac{3 \ln(t/t_0)}{8\pi D_f \Lambda^{f-2}(1+f)t} \left(\frac{t}{t_0} \right)^{-\frac{2-f}{1+f}} \tag{26}$$

In the present case, unlike with the action of section II, the strength of disorder affects the decay exponent significantly. The relationship between the decay exponent and γ is plotted in Fig. 5. We see that a small amount of potential disorder leads to an increased rate of reaction in the Lévy flights. But as the potential disorder increases further, the rate of reaction eventually decreases. This figure is very much similar to the one that showed up in the study of reactive turbulent flow [9]. In fact, if the Lévy flight parameters are related to the turbulence parameters [9] as $f = 2 - g_\sigma^*$ and $\gamma = 4\pi D_f^2 g_\gamma^*$, these two models predict *exactly* the same concentration decays. As suggested in [9], in order for the reaction to occur, multiple reactants must be trapped in regions of low potential energy. After the trapped reactants are depleted, new reactants must be replenished by rapid transport to continue the reaction. Certain combinations of fast transport, $f < 2$, and disorder, γ , lead to 'superfast' reaction, $\alpha > 1$, as shown in Fig. 5. Interestingly, this result means that the inhomogeneous system can have a faster reaction rate than the homogeneous, well-mixed system.

IV. CONCLUSION

We have analyzed the $A + A \rightarrow \emptyset$ reaction in two dimensional Lévy flight systems using two models of random disorder. For a common model in the literature, the dynamic exponent always locks to the microscopic step

index f , and the reaction decay exponent varies between 1 and $2/f$. This surprisingly unphysical result that the disorder cannot slow down the reaction is due to the fact that this model does not satisfy detailed balance. For a model that does satisfy detailed balance, on the other hand, the disorder can and does modify the transport properties of the system. When the disorder is adjusted to be compatible with the Lévy flight statistics, the reaction decay exponent first rises above unity and then drops to zero as the strength of disorder is increased. These results are identical to those from reactive turbulent flow, and this harmony suggests that Lévy flights, properly interpreted, can be a viable model of turbulent fluid transport.

ACKNOWLEDGMENT

This research was supported by the Alfred P. Sloan Foundation through a fellowship to M.W.D.

- [1] D. Mollison, J. R. Stat. Soc. **39**, 283 (1977).
- [2] A. Ott, J. P. Bouchaud, D. Langevin, and W. Urbach, Phys. Rev. Lett. **65**, 2201 (1990).
- [3] J. Klafter, A. Blumen, G. Zumofne, and M. F. Shlesinger, Physica A **168**, 637 (1990).
- [4] H. C. Fogedby, Phys. Rev. E **58**, 1690 (1998).
- [5] J. Honkonen, Phys. Rev. E **53**, 327 (1996).
- [6] J. Honkonen, Phys. Rev. E **62**, 7811 (2000).
- [7] J.-M. Park and M. W. Deem, Phys. Rev. E **57**, 2681 (1998).
- [8] J.-M. Park and M. W. Deem, Phys. Rev. E **57**, 3618 (1998).
- [9] M. W. Deem and J.-M. Park, Phys. Rev. E **58**, 3223 (1998).
- [10] N. le Tran, J.-M. Park, and M. W. Deem, J. Phys. A: Math. Gen. **32**, 1407 (1999).
- [11] D. Vernon and M. Howard, Phys. Rev. E **63**, 041116 (2001).
- [12] B. P. Lee, J. Phys. A: Math. Gen. **27**, 2633 (1994).
- [13] V. E. Kravtsov, I. V. Lerner, and V. I. Yudson, J. Phys. A: Math. Gen. **18**, L703 (1985).
- [14] J. Zinn-Justin, *Quantum Field Theory and Critical Phenomena*, 3rd ed. (Clarendon Press, Oxford, 1996).